CrossMark

Sensitivity of the weather research and forecasting model to parameterization schemes for regional climate of Nile River Basin

Tebikachew Betru Tariku[1] · Thian Yew Gan[1]

Abstract Regional climate models (RCMs) have been used to simulate rainfall at relatively high spatial and temporal resolutions useful for sustainable water resources planning, design and management. In this study, the sensitivity of the RCM, weather research and forecasting (WRF), in modeling the regional climate of the Nile River Basin (NRB) was investigated using 31 combinations of different physical parameterization schemes which include cumulus (Cu), microphysics (MP), planetary boundary layer (PBL), land-surface model (LSM) and radiation (Ra) schemes. Using the European Centre for Medium-Range Weather Forecast (ECMWF) ERA-Interim reanalysis data as initial and lateral boundary conditions, WRF was configured to model the climate of NRB at a resolution of 36 km with 30 vertical levels. The 1999–2001 simulations using WRF were compared with satellite data combined with ground observation and the NCEP reanalysis data for 2 m surface air temperature (T2), rainfall, short- and longwave downward radiation at the surface (SWRAD, LWRAD). Overall, WRF simulated more accurate T2 and LWRAD (with correlation coefficients >0.8 and low root-mean-square error) than SWRAD and rainfall for the NRB. Further, the simulation of rainfall is more sensitive to PBL, Cu and MP schemes than other schemes of WRF. For example, WRF simulated less biased rainfall with Kain-Fritsch combined with MYJ than with YSU as the PBL scheme. The simulation of T2 is more sensitive to LSM and Ra than to Cu, PBL and MP schemes selected, SWRAD is more sensitive to MP and Ra than to Cu, LSM and PBL schemes, and LWRAD is more sensitive to LSM,

Ra and PBL than Cu, and MP schemes. In summary, the following combination of schemes simulated the most representative regional climate of NRB: WSM3 microphysics, KF cumulus, MYJ PBL, RRTM longwave radiation and Dudhia shortwave radiation schemes, and Noah LSM. The above configuration of WRF coupled to the Noah LSM has also been shown to simulate representative regional climate of NRB over 1980–2001 which include a combination of wet and dry years of the NRB.

Keywords WRF · Configuration of regional climate model · Temperature · Rainfall · Short and longwave radiation of Nile River Basin

1 Introduction

Global climate models (GCMs) are numerical climate models designed to simulate physical processes in the atmosphere, ocean, cryosphere and land surface at a global scale (IPCC-TGICA 2007). GCMs are the main tools for projecting future global climate in response to rising concentrations of greenhouse gases in the atmosphere. However, usually at a spatial grid resolution of 100–300 km, and daily temporal resolutions, the output of GCMs are generally too coarse for solving basin-scale, hydrologic and water resources management problems. As a result, climate data of GCMs needs to be downscaled to produce local or regional climate at resolutions useful for hydrologic applications. Coarse resolution climate data can be downscaled by statistical procedures or dynamically using regional climate models (RCM) to data of higher resolutions. In theory, a RCM designed to capture climate processes at basin scale can provide high resolution, representative climate data of river basins. For river basins with diversified climate and complex topography,

✉ Thian Yew Gan
  tgan@ualberta.ca

[1] Department of Civil and Environmental Engineering, University of Alberta, Edmonton AB T6G 1H9, Canada

such as the Nile river basin (NRB) with elongated ridges and escarpments parallel to faults of the East African Rift system, and the presence of large lakes such as Lake Victoria and Lake Tana (Pohl et al. 2011), high resolution climate data downscaled by a RCM from GCMs will be useful for the future management of such river basins, e.g., Mohamed et al. (2005) applied the regional atmospheric climate model (RACMO) to simulate the regional climate of the NRB. The socioeconomic activities and well-being of people living in most countries of the Nile basin are dependent on the rainfall and streamflow of the Nile River for water supply and for sustaining the agriculture via irrigation projects and/or rain-fed mechanism. However, climate change can potentially impact the rainfall variability and streamflow of NRB which could affect the reliability of NRB's water supply to its users. Therefore, high resolution climate data for NRB downscaled by a RCM from GCMs' climate projections will be useful to assess the potential impact of climate change to the future water resources of NRB.

Various RCMs have been developed to downscale coarse resolution climate data of GCMs or reanalysis data to fine resolution data for different river basins across the world. There have been regional climate modeling studies conducted for East Africa. For example, by fine tuning the cumulus convection schemes, radiative transfer formation, surface process, boundary layer physics, and lateral boundary conditions of the study domain using the regional climate model, version 2 (RegCM2), Sun et al. (1999a, b) simulated representative regional climate, e.g., major circulation, precipitation, temperature and water vapor patterns, of East Africa for October–December, 1988. Other studies conducted over East Africa using version 3 of the regional climate model (RegCM3) are such as Anyah et al. (2006), Anyah and Semazzi (2006, 2007), Segele et al. (2009a), and Diro et al. (2012). Furthermore, the RCM called weather research and forecasting (WRF) which has a wide range of physical parameterizations, has been applied to some parts of Africa, or the entire Africa (e.g., Pohl et al. 2011; Giorgi et al. 2009; Jones et al. 2011; Endris et al. 2013; Mooney et al. 2013; Flaounas et al. 2011). Since its development in 2000, WRF has been a popular RCM to simulate regional climate of various study sites across the world.

Pohl et al. (2011) examined WRF's simulations of the atmospheric water cycle of Equatorial East Africa using 58 combinations of physical parameterization, land-use categories, lateral forcing and the domain geometry. From the results, they found that the shortwave radiation scheme, the land surface model (LSM), the domain size, convective schemes and land-use categories play a more significant role than cloud microphysics, lateral forcing reanalysis, the number of vertical levels and planetary boundary layer (PBL) schemes in simulating reliable seasonal climate of Equatorial East Africa. The coordinated regional climate

downscaling experiment (CORDEX) (Giorgi et al. 2009; Jones et al. 2011), initiated by the World Climate Research Program, used WRF and other RCMs to simulate high-resolution (50 km) regional climate projections of different continents. Under CORDEX, Endris et al. (2013) evaluated the rainfall of East Africa simulated by ten different RCMs (including WRF), each set up with one set of model configuration and parameterizations. They found that most of RCMs simulated a reasonable pattern of rainfall climatology over the three sub-regions but with significant biases. Mooney et al. (2013) found that WRF could simulate the 2-m surface temperature of 1990–1995 over the European domain, CORDEX region-4, accurately. They found WRF to be most sensitive to LSMs, moderately sensitive to longwave radiation schemes, but not sensitive to microphysics and PBL schemes. In simulating precipitation, WRF is found to be more sensitive to LSMs in the summer than in the winter. However, precipitation simulated by WRF compared poorly with remotely sensed precipitation data.

Under CORDEX, Katragkou et al. (2015) evaluated the 1990–2008 regional climate simulated by WRF for the European domain using the ERA-Interim reanalysis data, in a multi-physics ensemble framework with different configurations of microphysics, convection and radiation schemes. They found a systematic bias in temperature and precipitation simulated by WRF for summer and winter, an over (under) simulation of the total cloud cover (downward shortwave radiation) over northern Europe, and a strong positive bias in the downward shortwave radiation in summer over central and southern Europe. For simulating the 2006 summer West Africa monsoon, Flaounas et al. (2011) examined the sensitivity of WRF to convection and PBL schemes. They found that temperature, vertical distribution of humidity, and rainfall amount simulated by WRF is very sensitive to PBL schemes, while the dynamics and variability of precipitation simulated are sensitive to convective parameterization schemes.

WRF is computationally expensive and its optimal performance requires a tedious investigation over different combinations of parameterization schemes which vary from region to region. To the best of our knowledge, only a few RCM studies have been tested over the NRB, and as far as we know, only CORDEX has done a limited test on the performance of WRF over the whole Africa which was set up as a single domain at 50 km resolution. The objective of this study is to fine tune the configuration and parameterization schemes of WRF so that it can simulate reliable regional climate of NRB for 1999–2001 using the ERA-Interim reanalysis data at 36 km resolution.

The paper is organized as follows: the brief description of regional climate model, configuration and study area are stated in Sect. 2. In Sect. 3, model verification methods for the simulated results are discussed. The results and

discussions of different evaluation are presented in Sect. 4. Finally, in Sect. 5, the conclusions of the study are presented.

2 Experimental setup

2.1 Model description and configuration

This study was conducted using the advanced weather research and forecasting regional climate model, version WRF 3.6.1. WRF is a nonhydrostatic, primitive-equation, mesoscale meteorological model with advanced climate dynamics, physics and numerical schemes. Detailed descriptions of the WRF can be found in the model manual of Skamarock et al. (2008) and also on the WRF user web site (http://www.mmm.ucar.edu/wrf/users). Like other RCMs, WRF tends to over or under-simulate the amount of rainfall, but it can capture essential features of storm events, such as the time of occurrence, evolution, duration and location of storms (Hong and Lee 2009; Chen et al. 2010). Possible factors contributed to this common shortcoming of climate models are such as uncertainties of initial conditions, limited knowledge on the rainfall generation process, cloud microphysics, numerical round-off errors, etc. (Fowle and Roebber 2003; Fritsch and Carbone 2004). However, the selection of schemes and fine tuning of parameters for various modules of WRF, domain configurations and grid resolutions play a major role in the performance of WRF.

In the pre-processing stage of WRF, we evaluated two land use databases, sea surface temperature, setting of vertical layers and relaxation zones for lateral boundaries of the study domain. WRF was finally set up with 30 vertical pressure levels and the top level is at 50 hPa. For the study period 1999–2001, the initial and lateral boundary conditions of WRF are based on the most recent, ERA-Interim reanalysis data of the European centre for Medium Range Weather Forecasts (ECMWF) at $0.25° \times 0.25°$ resolution and 6-h time steps. Compared with other reanalysis data, past studies show that the ERA-Interim data best represented certain aspects of the climate system, such as the air temperature (Mooney et al. 2011; Troy and Wood 2009; Screen and Simmonds 2011).

The parameterization schemes in WRF are grouped into these modules: (1) microphysics (MP), (2) longwave radiation (LW), (3) shortwave radiation (SW), (4) land surface model, (5) cumulus (Cu), and (6) planetary boundary layer. Each of these modules has two or more parameterization schemes, with some schemes more applicable for climate modeling while others for weather forecasting, or both, thus making WRF a popular RCM. In fine tuning WRF, because of computational constraint, we could only test a limited combination of all available parameterization schemes, instead of testing all possible combinations. The performance of WRF for modeling the regional climate of NRB is assessed by its ability to reproduce the spatial and temporal patterns of the observed climate of NRB. 31 combinations of schemes selected to fine tune WRF over NRB are shown in Table 1. These schemes were selected either because they performed well in previous studies or they have not been tested before (Pohl et al. 2011; CORDEX Africa groups). Out of 31 experiments, 20 were conducted from combinations between 2 Cu, 2 PBL and 5 MP schemes, while 8 experiments were conducted from combining 2 Ra with 4 MP schemes; and 3 more experiments were conducted from combining 3 Ra schemes with 1 other LSM.

Since the dynamics and variability of precipitation are sensitive to convection parameterization schemes, two cumulus parameterization schemes, the Kain-Fritsch (KF) (Kain 2004) and Betts-Miller-Janjic (BMJ) (Janjic 1994) schemes were tested in this study. Even though it tends to overestimate the precipitation, the KF is the widely used cumulus parameterization scheme. Furthermore, the vertical distribution of temperature, humidity, and rainfall amount can be significantly affected by the PBL schemes. In this study, the popular Yonsei University (YSU) scheme (Hong et al. 2006) and the Mellor-Yamada-Janjic scheme (MYJ) (Janjic 1994) were tested.

For the microphysics, the WRF single moment three-class (WSM3) scheme (Hong et al. 2004), Lin et al. (1983) scheme, WRF Single-Moment 5-class scheme (WSM5) (Hong et al. 2004), Morrison double-moment scheme (Morrison et al. 2009) and WRF double-moment 5-class scheme (WDM6) (Lim and Hong 2010) were tested. The WSM3 is a simple, efficient scheme that considers ice and snow processes at mesoscale grid sizes. On the other side, WSM5 is marginally more sophisticated that also considers mixed-phase processes and super-cooled water. The radiation schemes tested were the Rapid Radiative Transfer Model (RRTM) LW scheme (Mlawer et al. 1997), Dudhia (1989) SW schemes, Community Atmosphere Model (CAM) (Collins et al. 2004) and a new version of RRTM (RRTMG) (Iacono et al. 2008) for both the LW and SW radiation schemes. Lastly, the two land surface models tested were the Noah (Ek and Mahrt 1991) and the rapid update cycle (RUC) (Smirnova et al. 1997, 2000). RUC is set up to simulate soil temperature and moisture for six layers, snow and frozen soil physics for multiple layers while the Noah LSM simulates soil temperature and moisture for four layers.

2.2 Domain configuration for the Nile River Basin

The Nile River is the longest river in the world with a length of 6800 km. It covers an area of about 3,400,000 km^2 and it flows over 11 countries (Burundi, DR Congo, Egypt, Eritrea, Ethiopia, Kenya, Rwanda, Tanzania, South Sudan, Sudan and Uganda). This study

Table 1 The combination of physical parameterization schemes for 31 WRF simulations

Experiment no.	Cu schemes	PBL	Microphysics	LW schemes	SW schemes	LSM
Test 1	KF	YSU	Lin	RRTM	Dudhia	NOAH
Test 2	BMJ					
Test 3	KF	MYJ				
Test 4	BMJ					
Test 5	KF	YSU	WSM3			
Test 6	BMJ					
Test 7	KF	MYJ				
Test 8	BMJ					
Test 9	KF	YSU	WSM5			
Test 10	BMJ					
Test 11	KF	MYJ				
Test 12	BMJ					
Test 13	KF	YSU	Morrison			
Test 14	BMJ					
Test 15	KF	MYJ				
Test 16	BMJ					
Test 17	KF	YSU	WDM5			
Test 18	BMJ					
Test 19	KF	MYJ				
Test 20	BMJ					
Test 21	KF	MYJ	WSM3	CAM	CAM	NOAH
Test 22			WSM5			
Test 23			Morrison			
Test 24			WDM5			
Test 25			WSM3	RRTMG	RRTMG	
Test 26			WSM5			
Test 27			Morrison			
Test 28			WDM5			
Test 29	KF	MYJ	WSM3	RRTM	Dudhia	RUC
Test 30				CAM	CAM	
Test 31				RRTMG	RRTMG	

will focus on the Blue Nile River (BNR) basin, which is a sub-basin of the Nile river basin. The drainage area of the BNR approximately covers an area of 210,000 km², but it contributes about 63% of the average annual flows of the Nile River. NRB has different rainy seasons with diverse climatic conditions ranging from arid, semi-arid to humid regions. From north to south, there are arid, tropical, and equatorial rainfall regimes. There is virtually no precipitation in the Sahara Desert of Sudan and Egypt, but precipitation increases southward to the Ethiopian highland and Equatorial Plateaus, with the June–September rainy season over Ethiopian plateau, and two rainy seasons over the Equatorial Lakes Plateau, October–December and March–May resulted from ITCZ moving southward and northward over the region, respectively. The southern part of the Nile basin has also one rainy season from October–December (Indeje et al. 2000; Nyakwada 2009; Endris et al. 2013). Because of different rainy seasons over the

NRB, WRF was set up to perform continuous simulation over each year of the study period. WRF was set up to simulate the climate of Nile over a two-domain's configuration with one-way nesting. Domain-1 (2°E–57°E, 20°S–37°N) was set up for the NRB and Domain-2 (29°E–45°E, 5°N–17.5°N) was set up for the BNR basin, as shown in Fig. 1. First, evaluation of different parameterization schemes was based on results obtained for Domain-1 (D1) only for 1999–2001. Then, WRF was run with Domian-2 (D2) nested within Domain-1 after we have obtained better parameterization schemes for Domain-1, to obtain results for both domains from 1980 to 2001. However, in this paper, only results obtained from testing D1 are presented. The ERA-Interim reanalysis data were used as the lateral boundary and initial conditions for D1 with a 36-km resolution. Then, the D1 output was used as lateral and initial conditions to run the inner domain D2 with a 12-km resolution. To account for sources of moisture coming from the
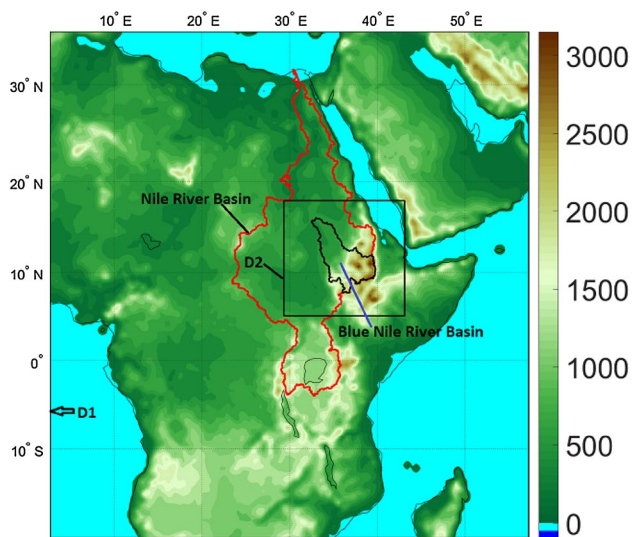
Fig. 1 A map showing the Domain-1 and Domain-2 setup of WRF and the topography (m) of the Nile and the Blue Nile River Basin of Africa

Atlantic and the Indian oceans, and to serve as a "spatial" spin-up, D1 was set up to be much wider than the NRB.

3 Model verification methods

The main problem in evaluating the performance of a RCM over Africa is a general lack of high-quality observation datasets of suitable temporal and spatial resolutions. The tropical rainfall measuring mission (TRMM 3B42 Version 6, 1998–2010) satellite based precipitation product with a 0.25° spatial and daily temporal resolutions were used to assess gridded precipitation simulated by WRF. Precipitation products of TRMM have been evaluated against rain gauge data in Africa, e.g., Nicholson et al. (2003a, b), Romilly and Gebremichael (2011), Mashingia et al. (2014). Even though TRMM data agree well with gauge data for most major climatic zones of Africa in all seasons (e.g., Adeyewa and Nakamura 2003), such satellite data have limitations, such as a lack of ability in capturing deep convective precipitation systems on daily timescales, particularly on the windward side of mountainous terrains (Dinku et al. 2008; Nair et al. 2009). In addition, two rain gauge-based datasets available at 0.5° spatial and monthly temporal resolutions, the Global Precipitation Climatology Centre (GPCC version 6, 1901–2010; Schneider et al. 2011) and the Climate Research Unit at the University of East Anglia (CRU version 3.22, 1901–2013; Harris et al. 2014) were also used to validate the simulation of WRF. Africa has a sparse network of rain gauges, and precipitation data interpolated from a sparse network of rain gauges could lead to large errors and

unrealistically smooth spatial gradients (Koutsouris et al. 2016). Therefore, we should be cautious using these widely used, gauge-based datasets. Nicholson et al. (2003a, b) used a dense network of rain gauge dataset to validate both the GPCP and the GPCC datasets for 1988–1994 and for 1998 over West Africa. They found that the mean precipitation fields derived from the dense gauge network, the GPCC and the GPCP are remarkably similar. However, they found that both GPCP and GPCC datasets compare well with the rain gauge data at seasonal but not at monthly time scales. The air temperature at 2 m (T2) simulated by WRF was evaluated against the CRU data; downward short- and longwave radiation at the surface simulated by WRF was evaluated against the National Centers for Environmental Prediction (NCEP) climate forecast system reanalysis (CFSR) data (Saha et al. 2010). The reanalyses data are climatological data generated from applying data assimilation schemes on available observed data into a climate model. Zhang et al. (2013) found that the latest reanalysis dataset called CFSR yields the best results in the precipitation mean and variability over South Africa when compared with the CRU data. In this study, the above observed and reanalysis data were re-gridded to the resolution of D1 to facilitate comparison with WRF's simulations. Some errors are expected in the re-gridding process, but the error introduced should not be significant, which will partly depend on the spatial variability of data and partly on the re-gridding algorithms used. The performance of WRF is assessed using statistics such as the root mean square error (RMSE), the mean error (ME) and the standard deviation (SD) calculated from all the simulations of WRF for each grid point of D1 over the study period; and the correlation coefficients between simulated and observed monthly climate variables. The spatial plots are used to evaluate the ability of WRF to capture the spatial distribution and the bias of WRF's simulations over the basins. These plots show different bias of WRF in different areas, but it is difficult to conclude if the overall bias for the entire basin is positive or negative. The time series of WRF's grid-based simulations for the BNR are spatially averaged and analysed to assess the ability of WRF to capture the rainfall seasonality of the BNR basin.

4 Results and discussions

4.1 Rainfall climatology

Figures 2 and 3 shows the mean annual rainfall bias in mm/day for all model configurations of WRF tested with respect to the TRMM datasets over the 1999–2001 period. We chose TRMM instead of GPCC data for comparison partly because TRMM datasets are of daily rainfall while GPCC are monthly rainfall data. Figure 2 presents the results using
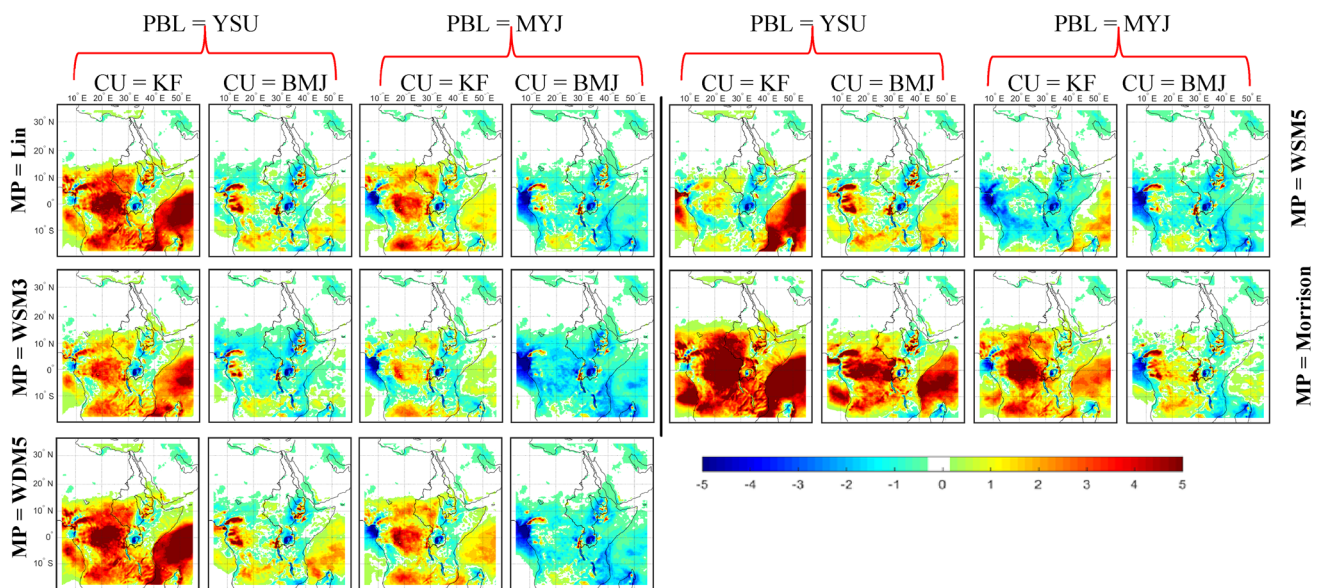
Fig. 2 Differences between observed (TRMM) and WRF's simulated annual mean rainfall (mm day^{-1}) over the Nile river basin under different MP, CU and PBL schemes, fixed RRTM, Dudhia Ra schemes and NOAH LSM
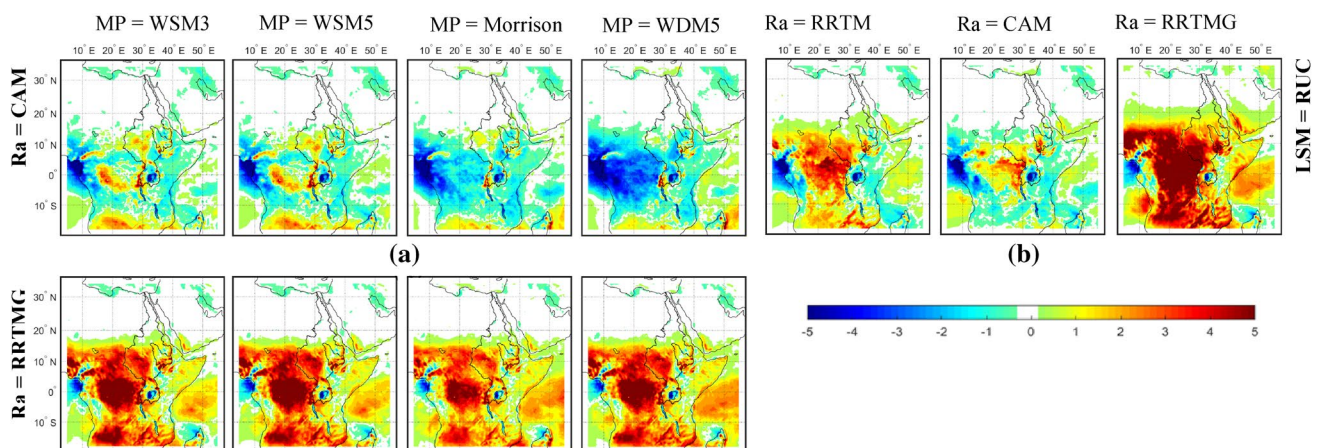

Fig. 3 Differences between observed (TRMM) and WRF's simulated annual mean rainfall (mm day^{-1}) over the Nile river basin under different combinations of (**a**) Ra and MP, with fixed MYJ and KF schemes, and NOAH LSM, and (**b**) Ra with fixed WSM3, MYJ, KF schemes, and RUC LSM

different combinations of WRF's parameterization schemes, which are cumulus parameterization (KF and BMJ), planetary boundary layer (YSU and MYJ) and microphysics (Lin, WSM3, WSM5, Morrison and WDM6); to determine which set of schemes can simulate the most representative rainfall of NRB, e.g., the depth and variability of rainfall. From these two figures, it seems that WRF simulated representative rainfall over the NRB in all parameterization schemes tested, but more schemes over-simulated while a few under-simulated the rainfall of Ethiopian highlands and the Congo basin, but most schemes under-simulated the rainfall over the Lake Victoria area. Other studies such as Endris et al.

(2013) also encountered this over-simulation problem over the Congo basin and Ethiopian highlands. The parameterization schemes considered consists of two cumulus parameterizations which controls the dynamics and variability of rainfall regimes are shown in columns 1 and 2 under the YSU PBL scheme; and columns 3 and 4 under the MYJ PBL scheme. Overall, KF tends to over-simulate rainfall while the BMJ scheme tends to under-simulate. Our results are consistent with that of Pohl et al. (2011), who also found KF to simulate a wetter climate than the BMJ scheme for East Africa. Figure 2 also shows that under KF combined with the YSU PBL scheme, WRF consistently over-simulated the

rainfall of the Indian Ocean and the eastern Congo Basin. Further, under a given set of PBL and Cu, the double-moment MP scheme would lead to more simulated rainfall than the single-moment MP, especially if KF is the cumulus scheme selected. In contrast, under the BMJ cumulus scheme, the effect of changing MP on the amount of rainfall simulated tends to be negligible. On a whole, the Morrison double-moment scheme is associated with more simulated rainfall, which also agrees with results of Pohl et al. (2011). The BMJ scheme is a moist convective adjustment scheme, where the thermodynamic profile is adjusted toward an observed reference profile in a quasi-equilibrium state. The BMJ scheme is triggered when the parcel is warmer than the environment determined by the convective available potential energy (CAPE). The scheme favors activation in cases with significant amounts of moisture at low and mid-levels and positive CAPE (Pohl et al. 2011). In contrast, KF, as a low-level control convective scheme, rearranges air mass in a column using the updraft, downdraft, and environmental mass fluxes until at least 90% of CAPE is removed (Kain 2004). The predominance of a strong convective regime over the Indian Ocean leads to over-simulation of rainfall.

Beside the cumulus scheme, by mixing and the transfer of surface water vapour to higher layers, PBL also plays a significant role in the amount of rainfall simulated. For example, the positive bias of KF over the Congo basin, Indian and Atlantic Ocean has been mostly corrected by changing the YSU PBL to the MYJ PBL scheme as shown in column 1 (YSU) and 3 (MYJ) of Fig. 2 under the KF Cu scheme. However, under MYJ, the rainfall of the West Coast of Africa/Cameroon tends to be under-simulated. In addition, combining MYJ PBL with the BMJ Cu scheme favours the simulation of a much drier climate compared with combining YSU PBL with BMJ Cu, which agrees with other studies, e.g., Evans et al. (2012) also found that YSU PBL tends to induce more convection in the KF scheme which leads to an over-simulation of precipitation. The MYJ (Mellor and Yamada 1982) tends to simulate a drier climate because it is a local closure PBL scheme reported to produce insufficient mixing in the convective boundary layer (Brown 1996), for a weaker vertical mixing would transfer less surface water vapour to higher layers (HU et al. 2010). In contrast, YSU (Hong et al. 2006) is a non-local closure PBL scheme that produces a well-mixed boundary layer profiles. This is likely a key reason why YSU favours a wetter simulation as compared with MYJ.

Besides PBL and Cu, the effect of different radiation schemes, which provides the atmospheric heating and the ground heat budget, over the amount of rainfall simulated, is shown in Fig. 3a. Figure 3a is presented with respect to different combinations of WRF's parameterization schemes, namely, radiation schemes (CAM and RRTMG) and microphysics (WSM3, WSM5, Morrison and WDM6) under KF and MYJ as the Cu and PBL schemes, respectively. Apparently, changing the radiation scheme than the MP scheme has a relatively larger effect on the amount of rainfall simulated, given that the RRTMG scheme generally leads to a wetter climate than other radiation schemes, especially the CAM scheme which tends to produce lesser rainfall.

Lastly, the LSM which interacts with the lower atmosphere also plays a role in the amount of moisture fluxes, the outgoing short- and longwave radiation and sensible heat fluxes simulated, which are partly absorbed by the cloud. This is because heat and moisture fluxes simulated by the LSM over the land surface will be used as the lower boundary conditions for computing the vertical transport in the PBL scheme (Skamarock et al. 2008). However, changing the LSM between Noah and RUC shows little effects over the amount of rainfall simulated as shown in Fig. 3b, even though RUC LSM marginally simulates more rainfall than the NOAH LSM (as shown in column-1 of Fig. 3a, and row-2 vs column-3 of Fig. 2).

The annual cycles of mean monthly rainfall for all test cases over the BNR basin are shown in Fig. 4. Compared with TRMM, CRU or GPCC dataset, more test cases show positive than negative bias during the May–September rainy season, but the simulations of WRF have generally captured the monthly rainfall variation of BNR/Ethiopian highland for the rainy season. As explained earlier, compared with the other parameterization schemes of WRF, under the KF cumulus with YSU PBL scheme, WRF tends to over-simulate the rainfall of BNR. A Taylor diagram is used to evaluate the agreement between the simulated and observed monthly rainfall using statistics such as the Pearson correlation, RMSE, and standard deviation for each simulation over the BNR basin as shown in Fig. 14a. The plot shows a relatively high correlation between simulated and TRMM data in monthly time step, but the standard deviations normalized by the standard deviation of TRMM tend to be larger than one, which means rainfall simulated by WRF show larger variabilities than satellite data. The RMSE of WRF's simulations range between 0.45 and 8.04 mm/day where higher RMSE represents simulations coming from WRF based on WSM3 MP, RRTMG radiation scheme, and RUC LSM.

4.2 Surface temperature at 2 m

Biases of the mean annual 2 m air temperature simulated by WRF under different parameterization schemes with respect to observed data of CRU are shown in Fig. 5. The results show that spatial patterns of temperature simulated by WRF generally agree well with observed data with reasonable discrepancies. Even though the maximum cold bias can be -7 °C and the maximum warm bias can be 8 °C at some places, the mean bias ranges from -3 to 0.5 °C. WRF clearly under-simulated the temperature of the Sahara Desert when
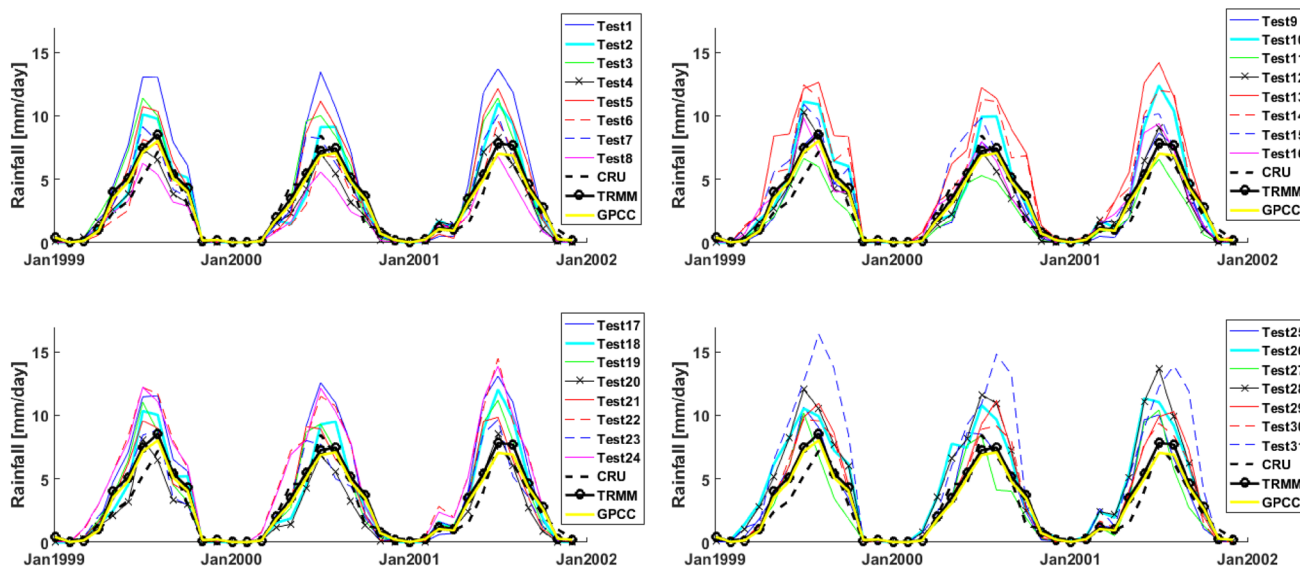
Fig. 4 Comparison of mean monthly rainfall (mm day^{-1}) simulated by WRF for Blue Nile River with observed data of CRU, TRMM, and GPCC
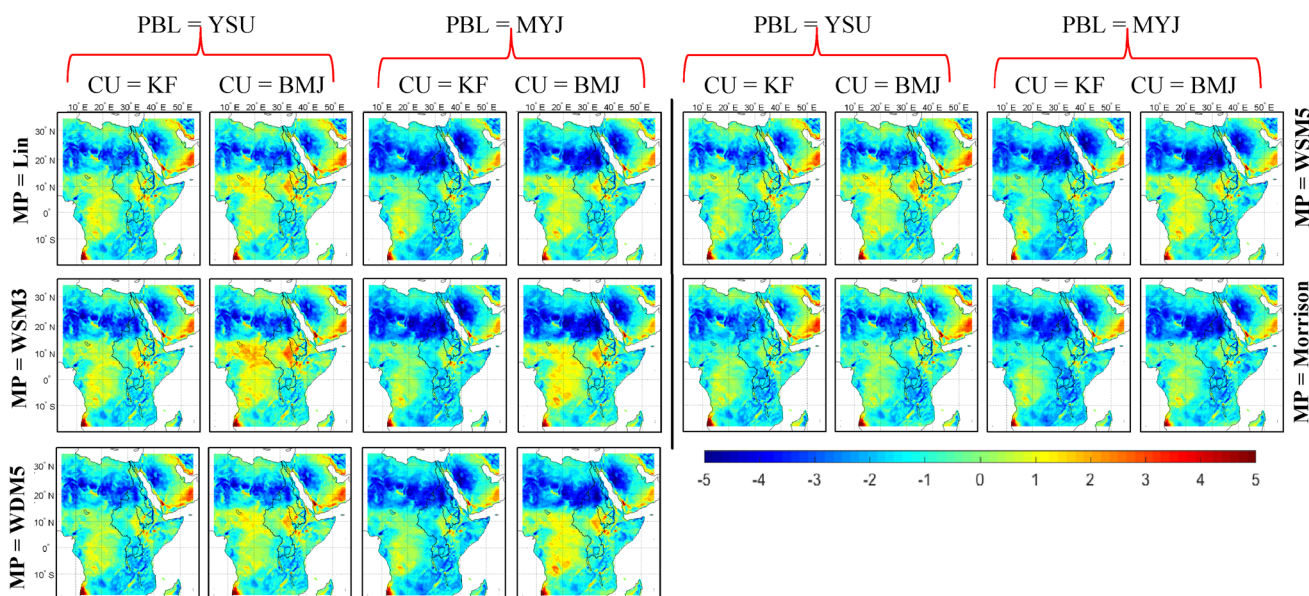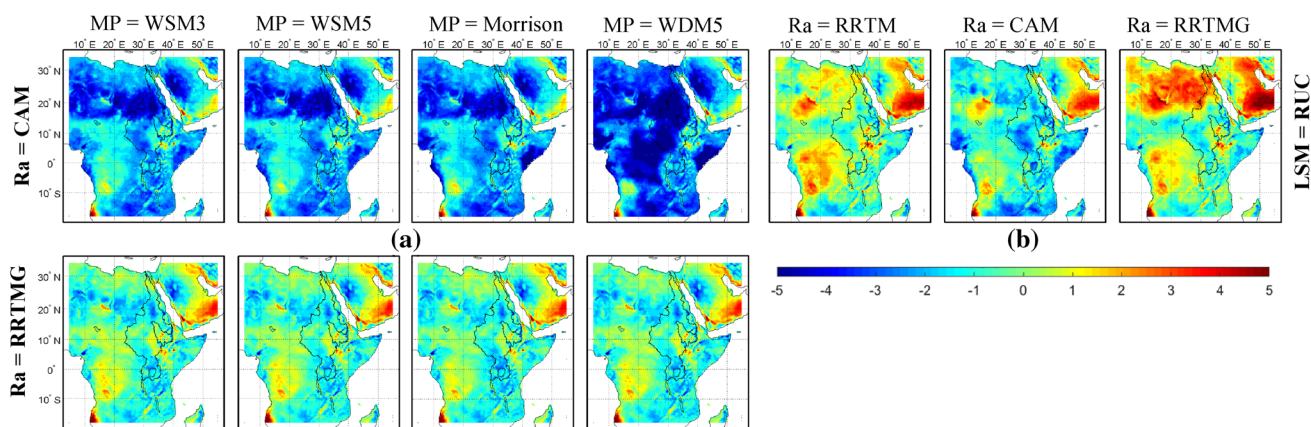

Fig. 5 Differences between observed (CRU) and WRF's simulated annual mean temperature (°C) over the Nile river basin under different combinations of MP, CU and PBL schemes, fixed RRTM, Dudhia Ra schemes and NOAH LSM

the Noah LSM was used, and even the NCEP reanalysis data is also too cold for the Sahara Desert when compared with the CRU data (not shown here). As a result, we cannot objectively assess the bias of temperature simulated by WRF under certain selected parameterization schemes with default parameters built into WRF, for as expected, observed data such as CRU also has uncertainties.

On the basis of differences between WRF's simulations and the CRU annual mean Temperature (°C) over the NRB

for different combinations of MP, Cu and PBL schemes, it seems these schemes have marginal influence on the temperature simulated by WRF as shown in Fig. 5. On the other hand, LSM and Ra schemes which simulate the radiation forcing and heat exchanges between the land surface and the atmosphere exert stronger impact on air temperature simulated by WRF as shown in Fig. 6. Temperature biases over the Sahara Desert were partly corrected by changing either the LSM or the Ra scheme. The RRTMG combined with

Fig. 6 Differences between observed (CRU) and WRF's simulated annual mean temperature (°C) over the Nile river basin under different combinations of (**a**) Ra and MP, with fixed MYJ and KF schemes, and NOAH LSM, and (**b**) Ra with fixed WSM3, MYJ, KF schemes, and RUC LSM

Noah LSM simulated more accurate air temperature compared to other radiation schemes as shown in Fig. 6a, while the CAM scheme resulted in a large negative temperature bias over the whole domain set up for the NRB. Also, using the RUC LSM resulted in a higher simulated temperature than the Noah LSM as shown in Fig. 6b. Similarly, Mooney et al. (2013) also found the summer surface temperature of Europe simulated by WRF was mostly controlled by the selection of land surface models (LSMs) and radiation schemes but less sensitive to MP and PBL. In their study, they found the NOAH LSM simulated surface temperature that better agree with the observed data than the RUC LSM, even though under NOAH the surface temperature tends to be under-simulated, especially when combining NOAH with the CAM radiation scheme.

Figure 7 shows the mean monthly, areally averaged 2 m air temperature of BNR basin simulated by WRF for all the test cases to generally capture the characteristic of observed temperature of BNR, with lower air temperature during rainy seasons than dry seasons. Among all test cases considered, the CAM radiation scheme combined with WDM6 MP (designated as Test 27) resulted in simulated air temperature that on a whole is colder than all other test cases conducted in this study. The RMSE of WRF's simulated temperature ranges from 0.27 to 4 °C, has a correlation with the observed temperature higher than 0.8, and the normalized standard
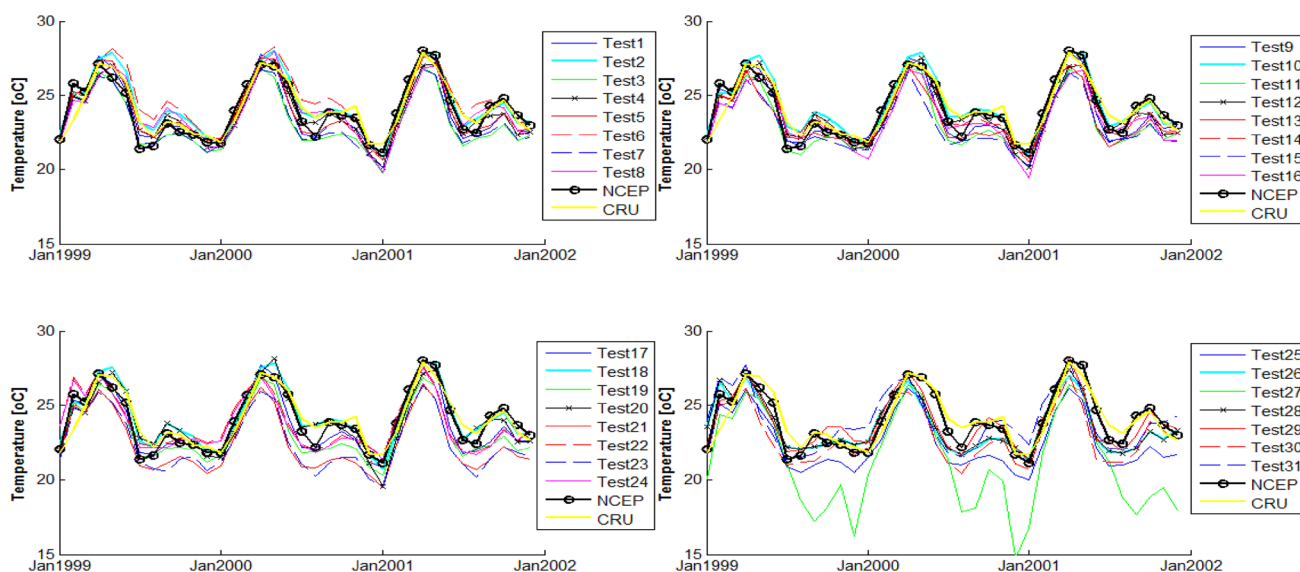
Fig. 7 Comparison of mean monthly 2 m temperature (°C) simulated by WRF for Blue Nile River with observed data of CRU and NCEP

deviation is closed to one as shown in Fig. 14b of the Taylor diagram.

4.3 Downward longwave radiation at the surface (LWRAD)

Figures 8 and 9 shows the mean annual surface downward longwave radiation bias (W.m^{-2}) for all model configurations of WRF tested with respect to NCEP reanalysis data. The LWRAD is less sensitive to Cu and MP schemes, but slightly more sensitive to Ra, LSM and PBL schemes as shown in Figs. 8 and 9. Under the YSU PBL scheme, RRTM simulated more LWRAD than under the MYJ PBL scheme.

Further, under the double-moment MP scheme RRTM simulated more LWRAD than under the single-moment MP, especially if YSU is the PBL scheme selected, e.g. the Morrison double-moment MP with YSU schemes lead to more LWRAD simulated than under other combination of MP and PBL schemes, resulting in higher rainfall simulated, as discussed in Sect. 4.1. Furthermore, in addition to Ra schemes, the selection of LSM also plays an important role in the amount of LWRAD as shown in Fig. 9. The figure shows that RUC LSM and RRTMG simulated larger LWRAD than other parameterization schemes of WRF considered in this study, while the CAM radiation scheme under-simulated LWRAD across the entire study domain. The discrepancy
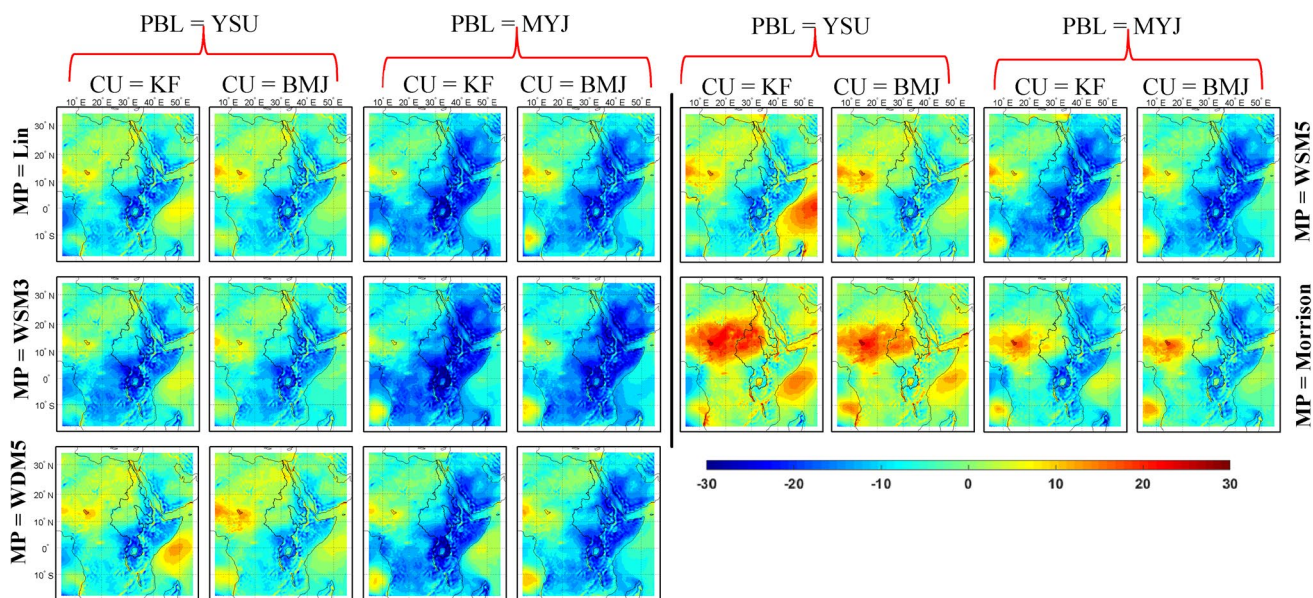
Fig. 8 Difference between NCEP reanalysis data and WRF`s simulated annual mean LWRAD (W.m^{-2}) over the Nile river basin for different combinations of MP, CU and PBL schemes, fixed RRTM, Dudhia Ra schemes and NOAH LSM
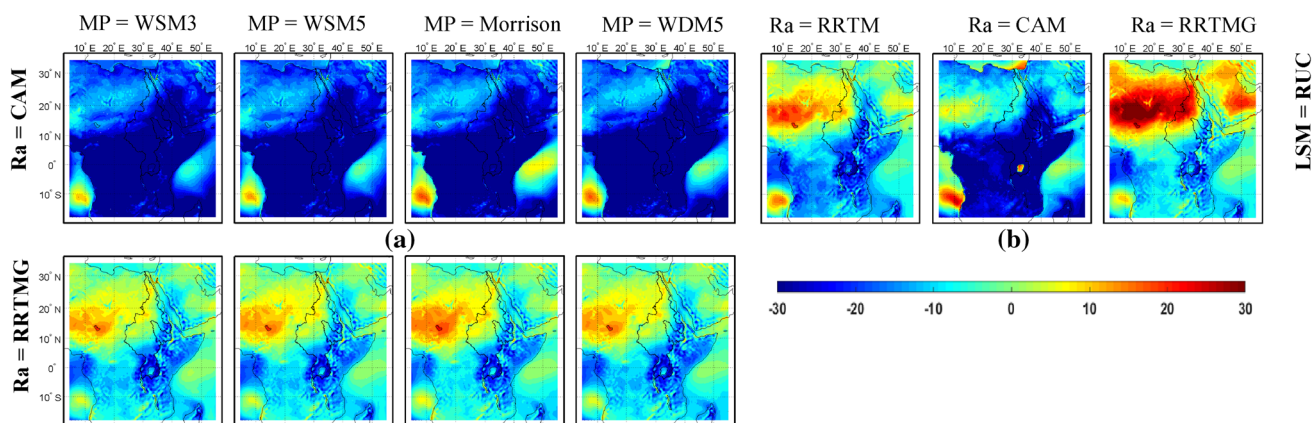
Fig. 9 Differences between annual mean LWRAD (W.m^{-2}) of NCEP reanalysis data and that simulated by WRF over the Nile river basin for different combinations of (**a**) Ra and MP, with fixed MYJ and KF schemes, and NOAH LSM, and (**b**) Ra with fixed WSM3, MYJ, KF schemes, and RUC LSM

between WRF's simulated LWRAD and that of NCEP reanalysis data under different combinations of parameterization schemes can range from −60 to 30 W.m^{-2}, and with a mean bias ranging from −25 to 3 W.m^{-2}, a RMSE ranging from 6.4 to 29.9 W.m^{-2}, and a standard deviation from 26.7 to 33.53 W.m^{-2}.

Figure 10 shows that in comparison to the NCEP data, the mean monthly, areally averaged LWRAD for the BNR basin simulated by WRF for all test cases suffers a systematic under-simulation, especially under the CAM radiation scheme. As shown in the Taylor diagram in Fig. 14c, the RMSE between the LWRAD of WRF and that of NCEP ranges from 25 to 134 W.m^{-2}, but their correlation is above 0.95, which demonstrates that the LWRAD simulated by WRF for the BNR basin with an acceptable uncertainty.

4.4 Downward shortwave radiation at the surface (SWRAD)

The downward shortwave radiation flux is dependent on the solar zenith angle which affects the path length. Further, while penetrating through the atmosphere, the SWRAD is attenuated by cloud covers, scattered by aerosols and dust particles, and also absorbed by atmospheric water-vapour. Besides SWRAD, the atmospheric cloud cover plays a critical role in the simulation of rainfall and LWRAD which are interconnected to each other. For example, more cloud cover means more rainfall but less SWRAD passing through the cloud which emits more LWRAD to the surface. Therefore, as shown in the figures, when LWRAD is under-simulated, rainfall is also expected to be under-simulated while SWRAD over-simulated, and vice versa, but this will also

depend on the cloud type and size, and the composition of water droplets and/or ice particles that form the cloud.

Biases in the mean annual SWRAD simulated by WRF with respect to the NCEP data are shown in Figs. 11 and 12. The annual rainfall of the Equatorial area, where SWRAD is mostly over-simulated by WRF, is higher than surrounding regions. Under the Dudhia shortwave radiation scheme, the simulation of SWRAD is less sensitive to Cu, PBL scheme and LSM, but very sensitive to the MP scheme. The higher the rainfall, the lesser will be the SWRAD simulated because of a higher absorption by cloud or water particles in the atmosphere. Compared with other MP schemes, the Morrison scheme is associated with over-simulated rainfall (Sect. 4.1) but the SWRAD simulated agrees better with the NCEP reanalysis data, while Lin and WSM3 MP schemes are associated with more bias in the SWRAD simulated. In terms of the radiation schemes, RRTMG and CAM generally simulate higher amount of SWRAD than the Dudhia scheme as shown in Fig. 12. On the other hand, in contrary with the Dudhia shortwave radiation scheme (shown in Fig. 11), under CAM and RRTMG radiation schemes, the effect of MP schemes on the simulation of SWRAD is relatively marginal. Compared with the NCEP reanalysis data, WRF generally shows more over than under-simulation of SWRAD, with a discrepancy ranging from −120 to 160 W.m^{-2}; and a mean bias ranging from 3.9 to 45.53 W.m^{-2}. Between WRF's simulation and the NCEP data, the RMSE ranges from 19.3 to 51.8 W.m^{-2} and the standard deviation from 25.2 to 44.6 W.m^{-2}. From the mean monthly surface downward shortwave radiation average over BNR basin shown in Fig. 13, there is a systematic over-simulation of SWRAD over the BNR except when WRF was under the Morrison or the WSM5 microphysics schemes combined with the KF,
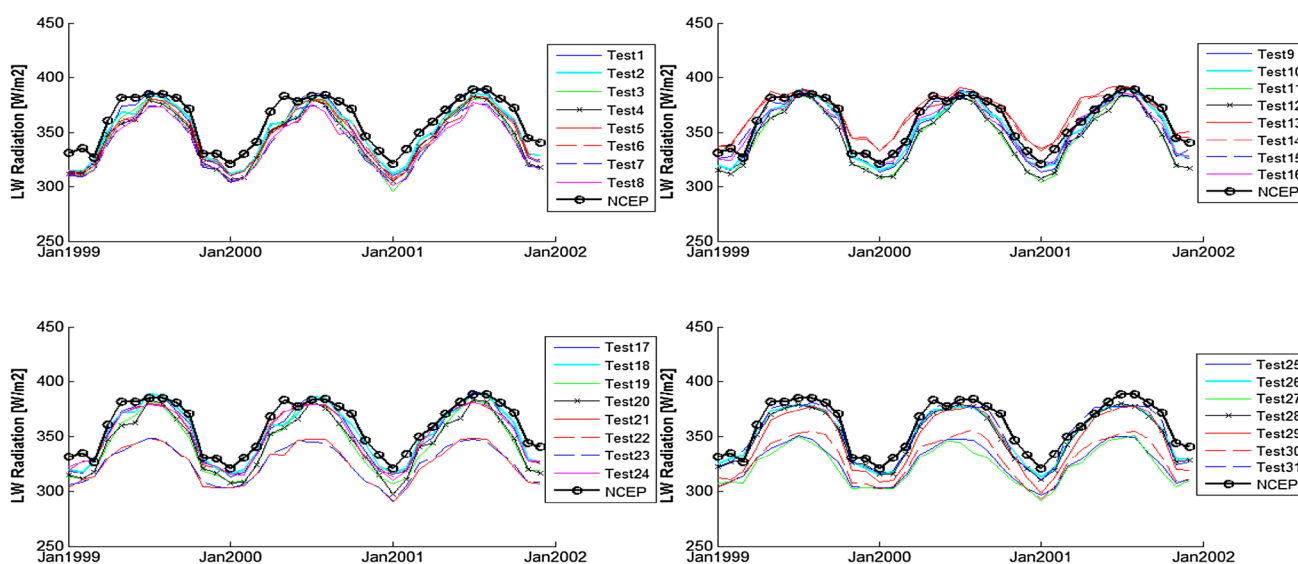

Fig. 10 Comparison of mean monthly LWRAD (W.m^{-2}) simulated by WRF for Blue Nile River with NCEP reanalysis data
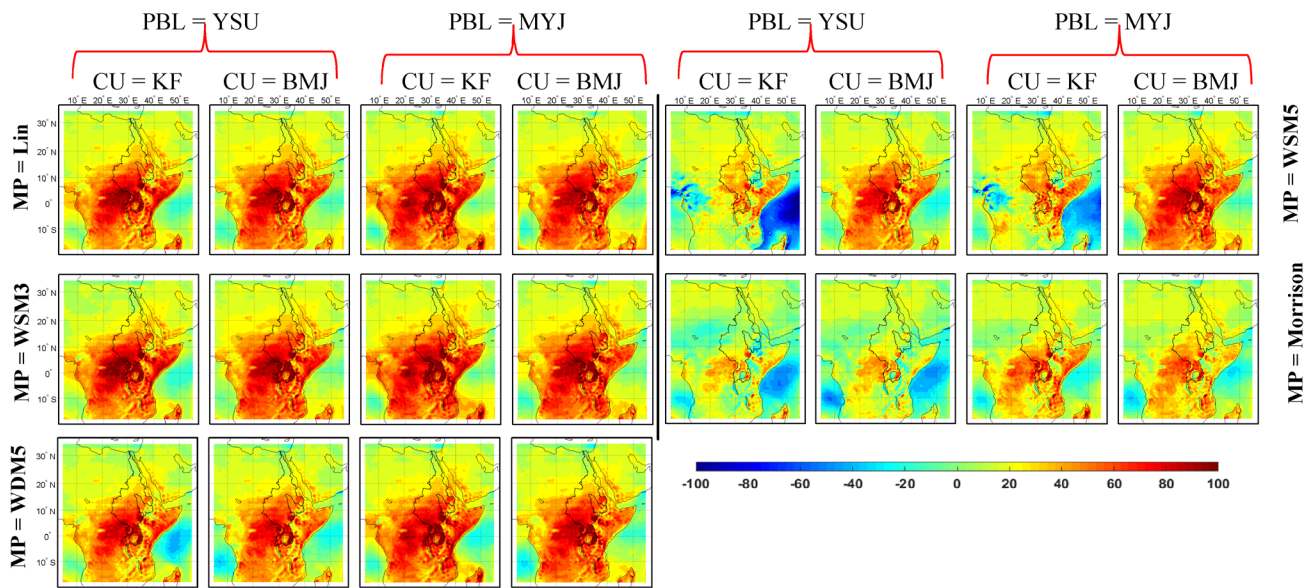
Fig. 11 Differences between NCEP reanalysis data and WRF`s simulated annual mean SWRAD (W.m^{-2}) over the Nile river basin under different combinations of Cu, MP and PBL, fixed RRTM, Dudhia Ra schemes and NOAH LSM
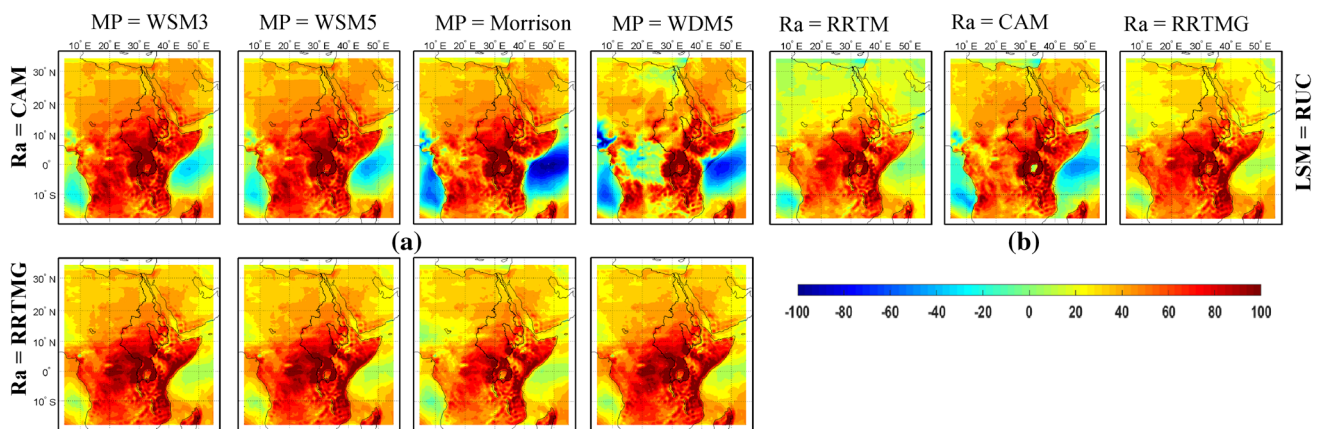

Fig. 12 Differences between NCEP reanalysis data and WRF's simulated annual mean SWRAD (W.m^{-2}) over the Nile river basin under different combination of (**a**) Ra and MP, with fixed MYJ and KF schemes, and NOAH LSM, and (**b**) Ra with fixed WSM3, MYJ, KF schemes, and RUC LSM

RRTM, and YSU schemes. The Taylor diagram of Fig. 14d shows that the correlation between WRF's simulation and the NCEP reanalysis data ranges from 0.45 to 0.9, and the RMSE from 22 to 60 W.m^{-2}.

4.5 Multi-year regional climate simulation of WRF

From the above analysis of results, it seems that WRF can achieve modeling more representative regional climate of NRB by using the WSM3 microphysics, KF cumulus, MYJ PBL, RRTM longwave radiation, and Dudhia shortwave radiation schemes and coupled to the Noah LSM than other schemes coupled to Noah or other land surface schemes.

The above configuration of WRF calibrated from using the 1999–2001 data was further tested to see if WRF-Noah can simulate representative, long-term regional climate of NRB over 1980–2001 which include a combination of wet and dry years. The mean annual difference between observed and WRF simulated rainfall, temperature, long- and short-wave radiation are shown in Fig. 15. The results confirm that the configured WRF-Noah can simulate the climate of NRB accurately, with a RMSE between simulated and observed data of 1.1 mm day^{-1}, 2.4 °C, 13.2 and 40.7 W. m^{-2}; and a mean error of 0.27 mm day^{-1}, -2 °C, -10.5 and 31.3 W.m^{-2}; and the spatial correlation of 0.89, 0.92, 0.97 and 0.61 for rainfall, temperature, longwave and shortwave
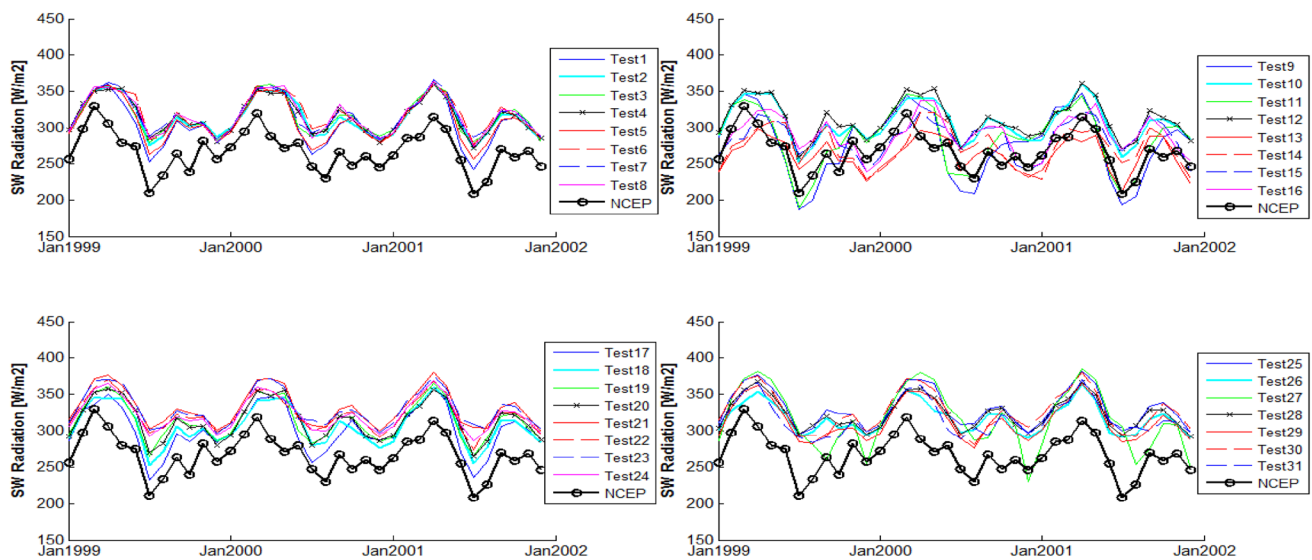
Fig. 13 Comparison of mean monthly SWRAD (W.m^{-2}) simulated by WRF for Blue Nile River with NCEP reanalysis data

radiation, respectively. Similar to results obtained for the 1999–2001 calibration experience, WRF over-simulated the rainfall in the Congo basin, under-simulated the temperature in the Sahara Desert, under-simulated the longwave radiation and over-simulated the shortwave radiation in NRB marginally. The long-term simulation of WRF was compared against NCEP reanalysis data for long- and shortwave radiation, and GPCC and CRU data for rainfall and temperature, respectively.

Figure 16 shows that the mean monthly, areally averaged rainfall, 2 m air temperature, long-, and shortwave radiation of BNR basin simulated by WRF for 1980–2001 generally captured the observed climate variables of BNR reasonably well, even though the rainfall of BNR was over-simulated during rainy season, and WRF consistently over- and under simulated the short- and longwave radiation of BNR, respectively. Comparing the rainfall, temperature, longwave and shortwave radiation simulated by WRF for BNR with the observed data, the correlations are 0.94, 0.91, 0.97, and 0.73; the RMSE are 1.14 mm day^{-1}, 1.13 °C, 21.4 and 61.5 W. m^{-2}; and the mean error are 0.29 mm day^{-1}, −0.82 °C, −20.4 and 58.3 W.m^{-2}, respectively. The above statistics between WRF's simulation with the observed climate data over the 1980–2001 period show that the configuration chosen for WRF coupled to the Noah LSM can reasonably simulate the long-term regional climate of BNR over both dry and wet years.

5 Summary and conclusions

In this study, WRF model was carefully configured to select the best optimal combination of parameterization schemes

to simulate representative, 1999–2001 climate of the NRB using ERA interim data as the boundary condition. As expected, no one parameterization scheme is consistently superior over other schemes under different evaluation criteria. In most RCM studies, the configuration and parameterization of a RCM is evaluated in terms of the accuracy of precipitation and temperature simulated only, which has its drawback because the results could be good even though the model configuration chosen may not be optimal for modeling a climatic regime. In this study using WRF as the RCM to model the regional climate of the NRB, the performance of WRF was also evaluated in terms of energy fluxes simulated, which should be more comprehensive than just evaluating WRF in terms of only precipitation and temperature simulated.

Overall, with reference to NCEP reanalysis and CRU climate data, the T2 and LWRAD simulated are generally more accurate than precipitation and SWRAD data for all WRF parameterization schemes tested in this study. The simulation of rainfall is more sensitive to the choice of PBL, Cu and MP schemes than other schemes of WRF. For example, combining the KF convective scheme with the YSU PBL scheme tends to simulate rainfall with significant bias over the NRB, while by combining KF with the MYJ PBL scheme, WRF simulated better rainfall than all other combinations of Cu and PBL schemes. T2 is more sensitive to LSM and Ra than to Cu, PBL and MP schemes selected for NRB. The surface air temperature simulated using Noah as the LSM agrees better with observed data (e.g., small negative bias) than that simulated using RUC as the LSM which has a high positive bias. From testing several radiation schemes with Noah as the LSM, the simulated T2 tends to have a negative bias with CAM as the radiation scheme, a positive bias with
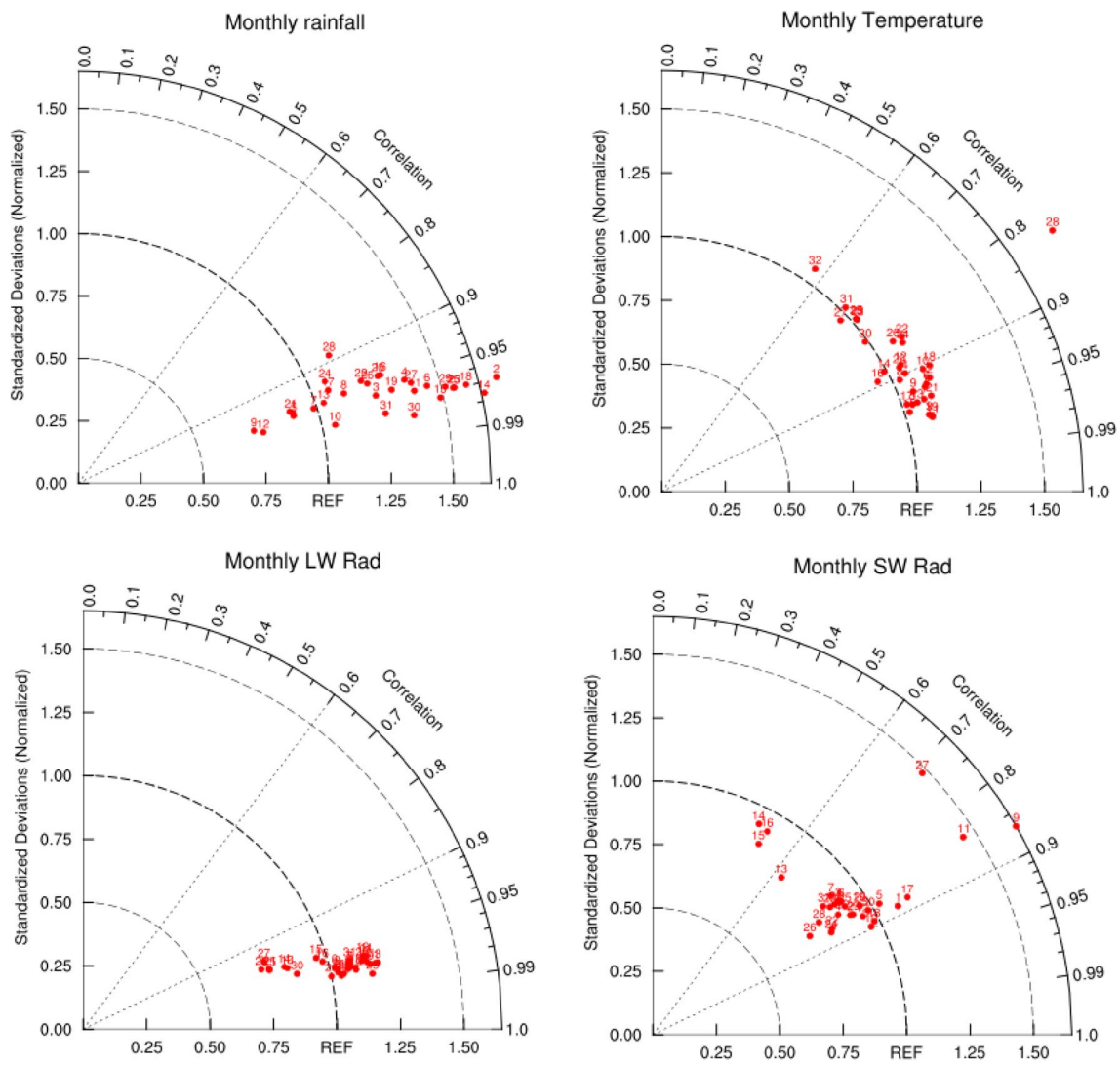
Fig. 14 Taylor diagram showing correlation coefficient and standard deviation of (**a**) mean monthly rainfall, (**b**) surface air temperature, (**c**) longwave radiation, and (**d**) shortwave radiation relative to observed and reanalysis data for the 31 WRF simulations over Blue Nile river basin
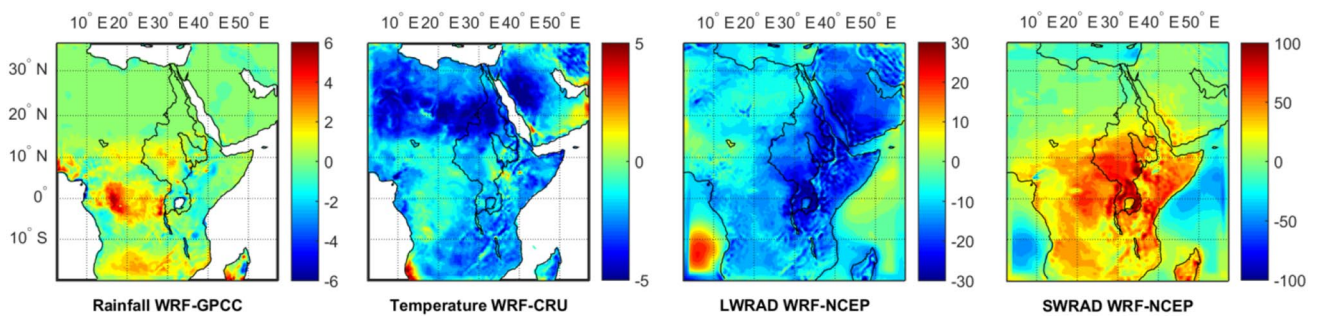

Fig. 15 Differences between observed GPCC, CRU, reanalysis NCEP data and WRF's simulated mean annual (1980–2001) rainfall, temperature, longwave and shortwave radiation over the Nile river basin
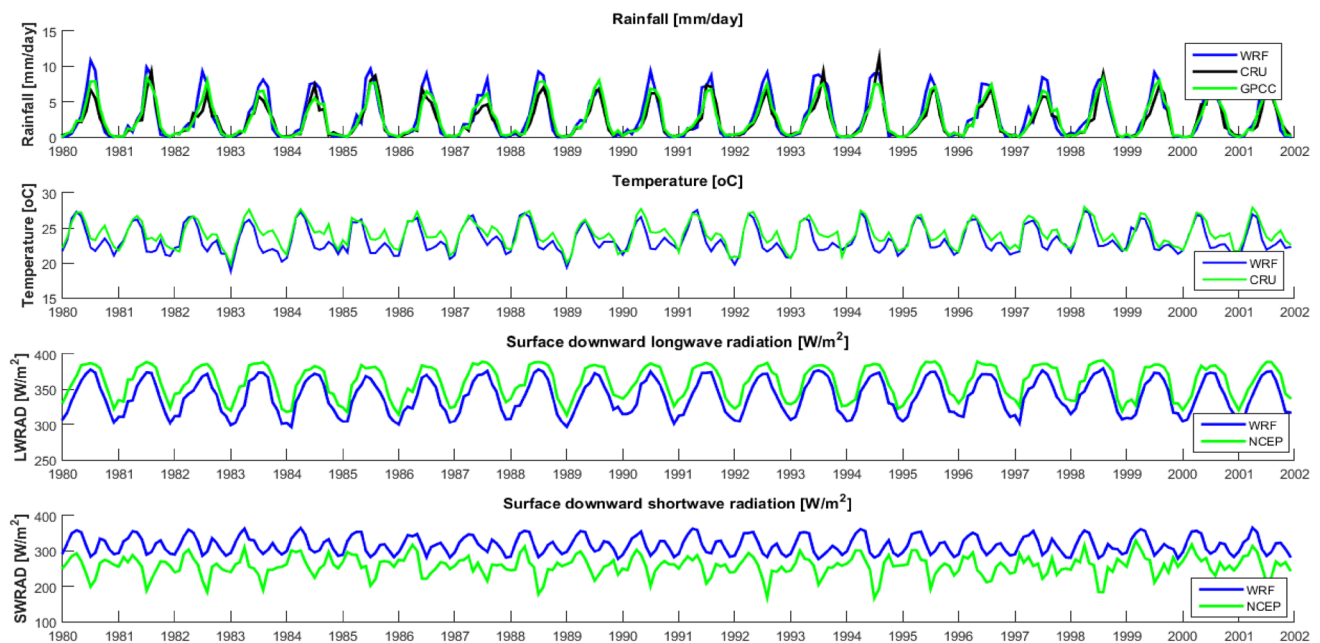
Fig. 16 Comparison of mean monthly rainfall, temperature, longwave, and shortwave radiation simulated by WRF for Blue Nile River with observed GPCC, CRU and NCEP radiation data

RRTMG as the radiation scheme, and has a negative bias over the Sahara Desert while using other radiation schemes. The SWRAD simulated by WRF is generally more dependent on MP and Ra schemes than Cu, LSM and PBL schemes. While most SWRAD simulated by WRF tends to have a positive bias, SWRAD simulated from combining the Morrison MP scheme with the Dudhia radiation scheme tends to be more accurate than other combination of schemes, e.g., SWRAD simulated from CAM and RRTMG schemes have more positive bias than that simulated using the Dudhia scheme. Finally, LWRAD simulated by WRF is highly sensitive to LSM, Ra and PBL schemes, but less sensitivity to Cu and MP schemes. On a whole, RUC, RRTMG and YSU schemes tend to result in simulating LWRAD with a positive bias than other schemes. Furthermore, with a strong positive bias in SWRAD, WRF tends to simulate low rainfall and low longwave radiation, and vice versa. Therefore, a careful selection of the configuration and physical parameterization schemes for WRF is essential to simulate representative key climate variables such as T2, precipitation, SWRAD and LWRAD. From a tedious effort calibrating WRF with the objective of simulating representative regional climate of NRB, we found the following combination of schemes to be more comprising than other schemes: the Single-moment WSM3 microphysics, KF cumulus, MYJ PBL, RRTM longwave radiation scheme, Dudhia shortwave radiation scheme, and Noah LSM. In addition, these selected schemes are also efficient in terms of computation time as compared with other WRF parameterization schemes tested in this study.

Lastly, the above configuration of WRF coupled to the Noah LSM has been shown to simulate representative regional climate of NRB over 1980–2001 which include a combination of wet and dry years of the NRB.

References

Adeyewa ZD, Nakamura K (2003) Validation of TRMM radar rainfall data over major climatic regions in Africa. J Appl Meteorol 42:331–347. doi:10.1175/1520-0450(2003)042<0331:VOTRRD>2.0.CO;2

Anyah RO, Semazzi FHM (2006) Climate variability over the Greater Horn of Africa based on NCAR AGCM ensemble. Theor Appl Climatol 86:39–62. doi:10.1007/s00704-005-0203-7

Anyah RO, Semazzi FHM (2007) Variability of East African rainfall based on multiyear RegCM3 simulations. Int J Climatol 27:357–371. doi:10.1002/joc.1401

Anyah RO, Semazzi FHM, Xie L (2006) Simulated physical mechanisms associated with multiscale climate variability over Lake Victoria Basin in East Africa. Mon Weather Rev 134:3588–3609. doi:10.1175/MWR3266.1

Brown AR (1996) Evaluation of parametrization schemes for the convective boundary layer using large-eddy simulation results. Bound Layer Meteor 81:167–200. doi:10.1007/BF00119064

Chen C-S, Lin Y-L, Peng W-C, Liu C-L (2010) Investigation of a heavy rainfall event over southwestern Taiwan associated with a subsynoptic cyclone during the 2003 Mei-Yu season. Atmos Res 95:235–254. doi:10.1016/j.atmosres.2009.10.003

Collins WD et al (2004) Description of the NCAR community atmosphere model (CAM3.0). Technical note TN-464+ STR, National Center for Atmospheric Research, Boulder, p. 214

Dinku T, Chidzambwa S, Ceccato P, Connor SJ, Ropelewski CF (2008) Validation of high resolution satellite rainfall products over complex terrain. Int J Remote Sens 29:4097–4110

Diro GT, Tompkins AM, Bi X (2012) Dynamical downscaling of ECMWF Ensemble seasonal forecasts over East Africa with RegCM3. J Geophys Res 117:D16103. doi:10.1029/2011JD016997

Dudhia J (1989) Numerical study of convection observed during the winter experiment using a mesoscale two-dimensional model. J Atmos Sci 46:3077–3107. doi:10.1175/1520-0469(1989)046<3077:NSOCOD>2.0.CO;2

Ek M, Mahrt L (1991) OSU 1-D PBL model user's guide, version 1.04. Department of Atmospheric Sciences, Oregon State University, Corvallis, p 120

Endris HS, Omondi P, Jain S et al (2013) Assessment of the performance of CORDEX regional climate models in simulating East African rainfall. J Clim 26:8453–8475. doi:10.1175/JCLI-D-12-00708.1

Evans JP, Ekström M, Ji F (2012) Evaluating the performance of a WRF physics ensemble over South-East Australia. Clim Dyn 39:1241–1258. doi:10.1007/s00382-011-1244-5

Flaounas E, Bastin S, Janicot S (2011) Regional climate modelling of the 2006 West African monsoon: sensitivity to convection and planetary boundary layer parameterisation using WRF. Clim Dyn 36:1083–1105. doi:10.1007/s00382-010-0785-3

Fowle MA, Roebber PJ (2003) Short-range (0–48 h) numerical prediction of convective occurrence, mode,and location. Weather Forecast 18:782–794. doi:10.1175/1520-0434(2003)018<0782:SHNPOC>2.0.CO;2

Fritsch JM, Carbone RE (2004) Improving quantitative precipitation forecasts in the warm season: a USWRP research and development strategy. Bull Am Meteor Soc 85:955–965. doi:10.1175/BAMS-85-7-955

Giorgi F, Jones C, Asrar GR (2009) Addressing climate information needs at the regional level: the CORDEX framework. WMO Bull 58(3):175–183

Harris I, Jones PD, Osborn TJ, Lister DH (2014) Updated high-resolution grids of monthly climatic observations—the CRU TS3.10 Dataset. Int J Climatol 34:623–642. doi:10.1002/joc.3711

Hong SY, Lee JW (2009) Assessment of the WRF model in reproducing a flash-flood heavy rainfall event over Korea. Atmos Res 93:818–831. doi:10.1016/j.atmosres.2009.03.015

Hong SY, Dudhia J, Chen SH (2004) A revised approach to ice microphysical processes for the bulk parameterization of clouds and precipitation. Mon Weather Rev 132:103–120. doi:10.1175/1520-0493(2004)132<0103:ARATIM>2.0.CO;2

Hong SY, Noh Y, Dudhia J (2006) A new vertical diffusion package with an explicit treatment of entrainment processes. Mon Weather Rev 134:2318–2341. doi:10.1175/MWR3199.1

Hu X-M, Nielsen-Gammon JW, Zhang F (2010) Evaluation of three planetary boundary layer schemes in the WRF model. J Appl Meteor Climatol 49:1831–1844. doi:10.1175/2010JAMC2432.1

Iacono MJ, Delamere JS, Mlawer EJ, Shephard MW, Clough SA, Collins WD (2008) Radiative forcing by long-lived greenhouse gases: calculations with the AER radiative transfer models. J Geophys Res 113:D13103. doi:10.1029/2008JD009944

Indeje M, Semazzi HMF, Ogallo JL (2000) ENSO signal in East African rainfall seasons. Int J Climatol 20:19–46. doi:10.1002/(SICI)1097-0088(200001)20:1<19::AID-JOC449>3.0.CO;2-0

IPCC-TGICA (2007) General guidelines on the use of scenario data for climate impact and adaptation assessment. Version 2. Prepared by T.R. Carter on behalf of the intergovernmental panel on climate change, task group on data and scenario support for impact and climate assessment, p. 66

Janjic ZI (1994) The step-mountain eta coordinate model: further developments of the convection, viscous sublayer, and turbulence closure schemes. Mon Weather Rev 122:927–945. doi:10.1175/1520-0493(1994)122<0927:TSMECM>2.0.CO;2

Jones CG, Samuelsson P, Kjellström E (2011) Regional climate modelling at the Rossby Centre. Tellus A 63:1–3. doi:10.1111/j.1600-0870.2010.00491.x

Kain JS (2004) The Kain–Fritsch convective parameterization: an update. J Appl. Meteor 43:170–181. doi:10.1175/1520-0450(2004)043<0170:TKCPAU>2.0.CO;2

Katragkou E, Garcia-Diez M, Vautard R, Sobolowski S, Zanis P, Alexandri G, Cardoso RM, Colette A, Fernandez J, Gobiet A, Goergen K, Karacostas T, Knist S, Mayer S, Soares PMM, Pytharoulis I, Tegoulias I, Tsikerdekis A, Jacob D (2015) Regional climate hindcast simulations with EURO-CORDEX: evaluation of a WRF multi-physics ensemble. Geosci Model Dev 8:603–618. doi:10.5194/gmd-8-603-2015

Koutsouris AJ, Chen D, Lyon SW (2016) Comparing global precipitation data sets in eastern Africa: a case study of Kilombero Valley, Tanzania. Int J Climatol 36:2000–2014. doi:10.1002/joc.4476

Lim K-SS, Hong S-Y (2010) Development of an effective double-moment cloud microphysics scheme with prognostic cloud condensation nuclei (CCN) for weather and climate models. Mon Weather Rev 138:1587–1612. doi:10.1175/2009MWR2968.1

Lin YL, Rarley RD, Orville HD (1983) Bulk parameterization of the snowfield in a cloud model. J Clim Appl Meteor 22:1065–1092. doi:10.1175/1520-0450(1983)022<1065:BPOTSF>2.0.CO;2

Mashingia F, Mtalo F, Bruen M (2014) Validation of remotely sensed rainfall over major climatic regions in Northeast Tanzania. Phys Chem Earth Parts 67–69:55–63. doi:10.1016/j.pce.2013.09.013

Mellor GL, Yamada T (1982) Development of a turbulence closure model for geophysical fluid problems. Rev Geophys 20:851–875. doi:10.1029/RG020i004p00851

Mlawer EJ, Taubman SJ, Brown PD, Iacono MJ, Clough SA (1997) Radiative transfer for inhomogeneous atmosphere: RRTM, a validated correlated-k model for the long-wave. J Geophys Res 02:16663–16682. doi:10.1029/97JD00237

Mohamed YA, van den Hurk BJJM, Savenije HHG, Bastiaanssen WGM (2005) Hydroclimatology of the Nile: results from a regional climate model. Hydrol Earth Syst Sci 9:263–278. doi:10.5194/hess-9-263-2005

Mooney PA, Mulligan FJ, Fealy R (2011) Comparison of ERA-40, ERA-Interim and NCEP/NCAR reanalysis data with observed surface air temperatures over Ireland. Int J Climatol 31:545–557. doi:10.1002/joc.2098

Mooney PA, Mulligan FJ, Fealy R (2013) Evaluation of the sensitivity of the weather research and forecasting model to parameterization schemes for regional climates of Europe over the period 1990–1995. J Clim 26:1002–1017. doi:10.1175/JCLI-D-11-00676.1

Morrison H, Thompson G, Tatarskii V (2009) Impact of cloud microphysics on the development of trailing stratiform precipitation in a simulated squall line: comparison of one- and two moment schemes. Mon Weather Rev 137:991–1007. doi:10.1175/2008MWR2556.1

Nair S, Srinivasan G, Nemani R (2009) Evaluation of multi-satellite TRMM derived rainfall estimates over a western state of India. J Meteorol Soc Jpn 87:927–939. doi:10.2151/jmsj.87.927

Nicholson SE, Some B, McCollum J, Nelkin E, Klotter D, Berte Y, Diallo BM, Gaye I, Kpabeba G, Ndiaye O, Noukpozoun-kou JN, Tanu MM, Thiam A, Toure AA, Traore AK (2003a) Validation of TRMM and other rainfall estimates with a high-density gauge dataset for West Africa. Part II: validation of TRMM rainfall products. J Appl Meteorol 42:1355–1368. doi:10.1175/1520-0450(2003)042<1355:VOTAOR>2.0.CO;2

Nicholson SE, Some B, McCollum J, Nelkin E, Klotter D, Berte Y, Diallo BM, Gaye I, Kpabeba G, Ndiaye O, Noukpozounkou JN, Tanu MM, Thiam A, Toure AA, Traore AK (2003b) Validation of TRMM and other rainfall estimates with a high-density gauge dataset for West Africa. Part I: validation of GPCC rainfall product and pre-TRMM satellite and blended products. J Appl Meteorol 42:1337–1354. doi:10.1175/1520-0450(2003)042<1337:VOTAOR>2.0.CO;2

Nyakwada W (2009) Predictability of East African seasonal rainfall with sea surface temperature gradient modes, Ph.D. dissertation, University of Nairobi, pp 265

Pohl B, Cretat J, Camberlin P (2011) Testing WRF capability in simulating the atmospheric water cycle over Equatorial East Africa. Clim Dyn 37:1357–1379. doi:10.1007/s00382-011-1024-2

Romilly TG, Gebremichael M (2011) Evaluation of satellite rainfall estimates over Ethiopian river basins. Hydrol Earth Syst Sci 15:1505–1514. doi:10.5194/hess-15-1505-2011

Saha S et al (2010) NCEP climate forecast system reanalysis (CFSR) 6-h products, January 1979–December 2010. Research data archive at the National Center for Atmospheric Research, Computational and Information Systems Laboratory. http://dx.doi.org/10.5065/D69K487J. Accessed 20 Jul 2015

Schneider U, Becker A, Finger P, Meyer-Christoffer A, Rudolf B, Ziese M (2011) GPCC full data reanalysis version 6.0 at 0.5°: monthly land-surface precipitation from Rain-Gauges built on GTS-based and historic data. doi:10.5676/DWD_GPCC/FD_M_V6_050

Screen JA, Simmonds I (2011) Erroneous Arctic temperature trends in the ERA-40 reanalysis: a closer look. J Clim 24:2620–2627. doi:10.1175/2010JCLI4054.1

Segele ZT, Leslie LM, Lamb PJ (2009a) Evaluation and adaptation of a regional climate model for the Horn of Africa: rainfall climatology and interannual variability. Int J Climatol 29:47–65. doi:10.1002/joc.1681

Skamarock WC, Klemp JB, Dudhia J, Gill DO, Barker M, Duda MG, Huang XY, Wang W, Powers JG (2008) A description of the advanced research WRF version 3. NCAR technical note, NCAR/TN-475+STR, p 113. http://www2.mmm.ucar.edu/wrf/users/docs/arw_v3.pdf

Smirnova TG, Brown JM, Benjamin SG (1997) Performance of different soil model configurations in simulating ground surface temperature and surface fluxes. Mon Weather Rev 125:1870–1884 doi:10.1175/1520-0493(1997)125<1870:PODSMC>2.0.CO;2

Smirnova TG, Brown JM, Benjamin SG, Kim D (2000) Parameterization of cold season processes in the MAPS land surface scheme. J Geophys Res 105:4077–4086. doi:10.1029/1999JD901047

Sun L, Semazzi FHM, Giorgi F, Ogallo L (1999a) Application of the NCAR regional climate model to eastern Africa: 1. Simulation of the short rains of 1988. J Geophys Res 104(D6):6529–6548. doi:10.1029/1998JD200051

Sun L, Semazzi FHM, Giorgi F, Ogallo L (1999b) Application of the NCAR regional climate model to eastern Africa: 2. Simulation of interannual variability of short rains. J Geophys Res 104(D6):6549–6562. doi:10.1029/1998JD200050

Troy TJ, Wood EF (2009) Comparison and validation of gridded radiation products across northern Eurasia. Environ Res Lett 4:045008. doi:10.1088/1748-9326/4/4/045008

Zhang Q, Körnich H, Holmgren K (2013) How well do reanalyses represent the southern African precipitation? Clim Dyn 40:951. doi:10.1007/s00382-012-1423-z